Combining Tube Design and Simple Kinematic Strategy for Follow-the-Leader Deployment of Concentric Tube Robots

Cédric Girerd, Kanty Rabenorosoa, and Pierre Renaud

Abstract Concentric tube robots show promising performances for many medical applications. A particularly useful but challenging deployment of these robots, called "follow-the-leader" deployment, consists in the robot following the path traced out by its tip. In this paper, we propose to combine a simple and analytical kinematic approach combined with now possible tube design to offer efficient follow-the-leader behavior. The approach is presented and then assessed with promising performances using a realistic scenario in the context of human nose exploration.

Key words: Continuum robot, concentric tube robot, robot design, follow-the-leader kinematics.

1 Introduction

Concentric tube robots (CTR) constitute a class of continuum robots that is of particular interest in the medical context [3]. The displacements of the robot end-effector are then obtained by relative translations and rotations of precurved elastic tubes with diameters that can be typically below 3 mm [5, 8]. Complex shapes of robots can be generated using remote actuation, that is particularly relevant for navigation in constrained anatomical areas. CTR kinematics are however complex because of the mechanical interactions between the tubes. Several models have been derived that now include in particular the impact of tube torsion which occurs in the general case [2, 6]. Complementary work is now focused on the design of CTR tubes, with local modifications of their shape and structure to obtain anisotropic

Cédric Girerd and Pierre Renaud

ICube, UDS-CNRS-INSA, 300 bd Sébastien Brant - Illkirch, France. e-mail: cedric.girerd@icube.unistra.fr

Kanty Rabenorosoa

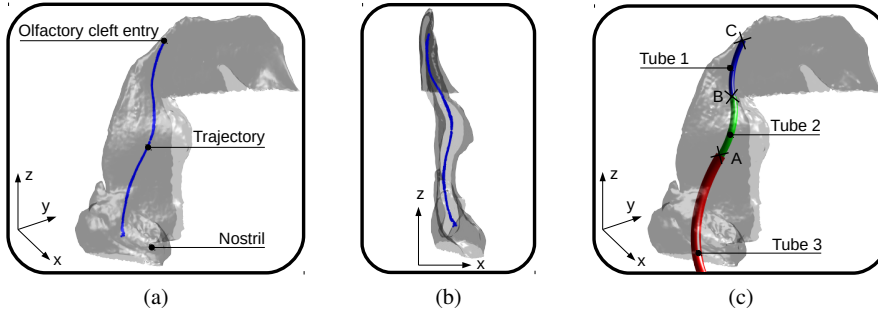FEMTO-ST, AS2M, Univ. Bourgogne Franche-Comté, UFC/ENSMM/CNRS, Besançon, France.

Fig. 1: Front view and perspective view of the nasal cavity with suitable trajectory (Fig. 1a, 1b) and CTR with 3 tubes deployed (Fig. 1c).

behavior and hence to modify the relative importance of bending and torsion in the tubes. Until now, it is however still difficult to build a CTR and its control to satisfy a so-called follow-the-leader approach, where the CTR body only occupies the volume swept by its tip during the deployment. Even though this approach can be mandatory from an application point-of-view, limited solutions have indeed been reported to choose accordingly a robot design, *i.e.* the number and geometry of precurved tubes, and the deployment sequence [6].

In this paper we propose a simple-to-use and yet efficient approach to CTR design, with the corresponding deployment strategy, that allows an approximate follow-the-leader behavior. In a realistic case study, *i.e.* the context of human nose exploration, it is shown to be of adequate performance. The design and deployment strategy combines the now existing possibility of tube design with a kinematic approach. For planar trajectories, the goal of the paper, analytical formulation of robot geometry, defined by number of tubes and their curvatures, and path following sequence are introduced. Required modifications of tubes are then determined from the task simulation. The method we propose consists first in path generation and robot design. Their descriptions are introduced in sections 2 and 3 respectively with illustration of the considered application. In section 4, the determination of tube modifications is performed and the method assessed through simulation of torsion impact as well as control errors during the deployment. Conclusions and perspectives are finally given in section 5.

2 Trajectory Generation

In [6], the conditions for exact follow-the-leader deployment have been investigated. To be admissible, a trajectory must not induce tube torsion. From a design point-of-view, tubes with precurved helical shapes are identified as candidates for such deployments, but their manufacturing remains delicate. The other option, for planar

paths, uses planar precured tubes with constant curvatures in the same or opposite configurations. As a first step of our method, the CTR path is hence determined by including this latter constraint. It can be easily demonstrated that a set of tubes with planar configurations and constant curvatures form a CTR with 2D shape and constant curvature by sections. The first step is therefore to identify a trajectory that is admissible from an application perspective and constituted by portions of constant curvatures.

In the following of the paper, an application is used for evaluation. We consider the deployment of a CTR to reach the olfactory cleft, located in the upper part of the nose. Fig. 1a represents the 3D shape of the area reconstructed from CT images. The goal is to reach the olfactory cleft starting from the nostril. A planar path with constant curvature by sections can be identified to join the two regions, as illustrated in Fig. 1a and 1b. A point-cloud extraction and circle-fitting algorithm based on least-squares optimization, not detailed for the sake of compactness, is used to identify the path parameters. Three sections are determined, with length and curvature for each one being equal to: 17.32, 14.27, 14.20 mm and 0.0353, 0.0646 and 0.0592 mm^{-1} respectively. The resulting trajectory is a key element that will be used as a reference to quantify deployment errors during the robot insertion.

3 Robot Design and Deployment

The CTR is considered to be composed of planar precured tubes of constant curvatures, located in the same plane, with aligned or opposite curvatures. In this situation indeed, no torsion occurs in the tubes. If the tubes have aligned curvatures, one can easily imagine that the resulting robot will be in a stable configuration. On the contrary, depending on tube mechanical properties, opposite curvatures can make the configuration unstable. This can be of course a main issue for the deployment. To handle this situation, modification of the tube structure as described in [1, 7] is considered. This does not affect the robot synthesis, described below, with determination of the number of tubes and their overall shapes, lengths and curvatures. Robot design is thus described below, tube design being introduced in section 4.

Let n be the number of tubes of the CTR. Each tube numbered i is described by its precurvature $\boldsymbol{u}_i^{*F_i(s)}(s) = [u_{ix}^*(s)\ u_{iy}^*(s)\ u_{iz}^*(s)]^T$ expressed in its cross section material coordinate frame $F_i(s)$. The stiffness properties of the tube are expressed by the frame-invariant stiffness tensor $K_i = \mathrm{diag}(E_i I_i, E_i I_i, G_i J_i)$, with E_i, G_i respectively its Young and Shear modulus, and I_i, J_i respectively its cross section area and polar moment of inertia. The curvature resulting from the combination of the n tubes is then given by [5]:

$$\boldsymbol{u}^{F_0(s)}(s) = \left(\sum_{i=1}^{n} K_i\right)^{-1} \sum_{i=1}^{n} K_i \boldsymbol{u}_i^{*F_0(s)}(s) \tag{1}$$

with $F_0(s)$ the cross-section reference frame which experiences no twist when translated along the robot's centerline.

In order to determine the robot geometry, we propose to invert Eq. (1) in order to solve for the tube curvatures. As the tubes are considered to have a constant curvature along their length, without any presence of torsion, their curvatures can then be written as $\boldsymbol{u}_i^* = [\kappa_i\,0\,0]^T$ or $\boldsymbol{u}_i^* = [0\,\kappa_i\,0]^T$. The path sections are characterized by their lengths $(s_1,\ldots,s_n)$ and curvatures $(1/r_1,\ldots,1/r_n)$, starting from the path end. The number n of tubes is immediately determined to correspond to the number of constant curvature sections on the path generated in the previous section. The tube lengths $(l_1,\ldots,ln)$ and curvatures $(\kappa_1,\ldots,\kappa_n)$ can then be determined using Eq. (2), which has to be solved first for tube 1, the inner tube, up to tube n, the outer tube, in increasing index order, and using positive or negative path and robot curvatures depending on the curvature direction:

$$l_j = \sum_{i=j}^{n} s_i$$

$$\kappa_1 = \frac{1}{r_1} \quad \text{and} \quad \kappa_{j,j>1} = \frac{1}{E_j I_j}\left(\sum_{i=1}^{j}\frac{E_i I_i}{r_j} - \sum_{i=1}^{j-1} E_i I_i \kappa_i\right) \tag{2}$$

In (2), the values of Young's modulus and cross section area moments of inertia I_j are chosen from characteristics of circular Nitinol tubes, the standard choice for CTR because of the material superelasticity. Using diameters of commercially-available circular tubes, the lengths and curvatures are obtained from Eq (2) and indicated in Table 1.

By extending the strategy described in [6], the computed CTR geometry can be deployed with a follow-the-leader approach. As a first step, the n tubes are inserted altogether by pure translation until the tube n reaches the end of its stroke (Fig. 2). Then, the $n-1$ tubes are inserted together, with the tube n remaining fixed, until tube $n-1$ reaches the end of its stroke. The procedure is repeated until the robot is fully deployed.
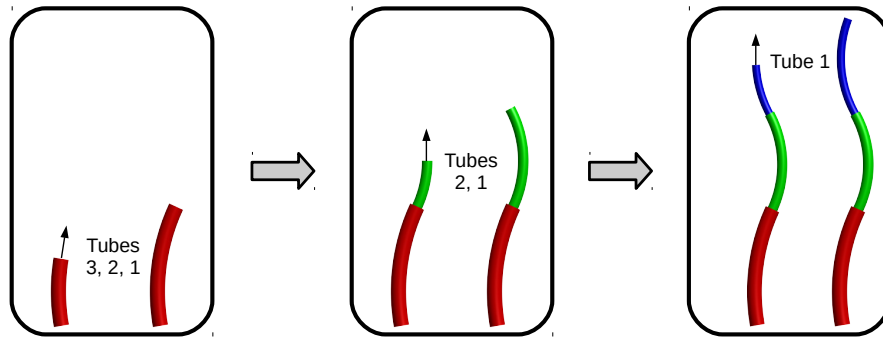

Fig. 2: Deployment sequence of CTR with three tubes ($n=3$)

Tube index	Young's modulus (GPa)	Shear modulus (GPa)	Inner diameter (mm)	Outer diameter (mm)	Length (mm)	Curvature (mm^{-1})
1	80	30	0.880	1.200	45.8	0.059
2	80	30	1.296	1.524	31.6	0.136
3	80	30	1.760	2.184	17.3	0.066

Table 1: Robot parameters after synthesis with the proposed method for the considered application.

4 Tube Design and Deployment Assessment

We have introduced in sections 2 and 3 how it is possible to generate a CTR geometry and its deployment strategy for planar paths composed of constant curvature sections. It was previously outlined that the use of concentric tubes with opposite curvatures can lead to unstable configurations. To make use of a CTR for medical purposes, it is obvious that only stable equilibrium positions should be used. In this section, we propose to design tubes with anisotropic properties by local structure modification to handle this particular issue and make the deployment strategy safe and accurate.

4.1 Robot kinematic model

The evaluation of the influence of tube properties is conducted using the application data. The presented application context will also be used to assess the deployment accuracy. Therefore, a model is needed to analyze the impact of torsion on the interactions between the tubes, and possible deviations between stable and unstable configurations. We here use the torsional model developed in [4, 10], based on an energy method. For a set of n tubes experiencing bending and torsion, the energy stored in the tubes is given by Eq. (3) if the tubes overlap continuously for $s \in [\sigma_1, \sigma_2]$.

$$E = \frac{1}{2} \int_{\sigma 1}^{\sigma 2} (\boldsymbol{u}(s) - \boldsymbol{\alpha}(s))^T K (\boldsymbol{u}(s) - \boldsymbol{\alpha}(s)) + C ds, \tag{3}$$

with

$$\boldsymbol{\alpha}(s) = K^{-1} \sum_{i=1}^{n} K_i \overline{\boldsymbol{u}}_i^*(s), \qquad K = \sum_{i=1}^{n} K_i, \qquad \theta_i(s) = \psi_i(s) - \psi_1(s),$$

$$\overline{\boldsymbol{u}}_i^*(s) = R_{\theta_i} \boldsymbol{u}_i^* - \dot{\theta}_i(s) \boldsymbol{e}_3, \qquad C(s) = \sum_{i=1}^{n} \overline{\boldsymbol{u}}_i^{*T}(s) K_i \overline{\boldsymbol{u}}_i^*(s) - \boldsymbol{\alpha}^T(s) K \boldsymbol{\alpha}(s), \tag{4}$$

In these equations, $\boldsymbol{u}(s)$ represents the equilibrium curvature vector for the robot, and R_{θ_i} the rotation matrix of angle θ_i about $\boldsymbol{e}_3 = [0\ 0\ 1]^T$. The angles $(\psi_1, \ldots, \psi_n)$ designate the absolute angular variables of each tube. As neither $C(s)$ nor $\boldsymbol{\alpha}(s)$

depends on $\boldsymbol{u}(s)$, the minimal energy is obtained for $\boldsymbol{u}(s) = \boldsymbol{\alpha}(s)$. In order to compute $\boldsymbol{\alpha}(s)$, the variables $\psi_i(s)$ that describe the evolution of torsion along the tubes have to be estimated. For tubes with constant curvature of the form $\boldsymbol{u}_i^* = [\kappa_i \ 0 \ 0]^T$ or $\boldsymbol{u}_i^* = [0 \ \kappa_i \ 0]^T$, as previously considered, functions $\psi_i(s)$ can be expressed by solving the system (5) of two first order differential equations [9]:

$$
\begin{aligned}
\dot{\psi}_i(s) &= u_{iz}(s) \\
\dot{u}_{iz}(s) &= \frac{E_i I_i}{EI G_i J_i} \sum_{j=1}^{n} E_j I_j \kappa_i \kappa_j \sin(\psi_i(s) - \psi_j(s))
\end{aligned}
\tag{5}
$$

where $EI = \sum_{j=1}^{n} E_j I_j$. The system (5) can be easily used for a CTR composed of several sections by writing it for each set of overlapped tubes and adding continuity constraints to the solution.

The set of equations representing torsion along the entire length of the robot is a boundary value problem that is solved numerically using a finite difference code as implemented in the bvp5c function in Matlab (The MathWorks Inc., Natick, USA). Boundary conditions are $\psi_i(0)$, the known angles at the tubes insertion points, and $\dot{\psi}_i(l_i) = 0$ as tubes can not apply axial moments at their distal ends. Finally, the shape of the robot can be determined using Eq. (6), with superscript symbol "hat" denoting the conversion of an element of $\mathbb{R}^3$ to an element of $\mathfrak{so}(3)$, the Lie algebra of Lie group SO(3).

$$
\begin{aligned}
\dot{\boldsymbol{p}} &= R\boldsymbol{e}_3 \\
\dot{R} &= R\hat{\boldsymbol{u}}
\end{aligned}
\tag{6}
$$

To solve Eq. (6), $\boldsymbol{u}(s)$ can be approximated by constant values over a given step size, and then a Runge-Kutta method can be used for the resolution.

4.2 Tube design

At this point, all the tube characteristics are known except the polar moments of inertia J_j, $j \in [1, n]$. To select their adequate values, that can be adjusted by local tube modification as described in [7], the ratio between bending and torsion stiffnesses is being varied in simulation. The ratio λ is equal to $E_j I_j / G_j J_j$ [7] and is considered identical for all the tubes. As expected, Fig. 3 shows that lowest values of λ minimize the torsional effects and finally the position errors in stable configurations. However, it is challenging to obtain experimentally very low values for λ. In [7], the authors have successfully reached a value of 0.344. For our application, a ratio $\lambda = 0.348$ results in a tip error of 2.51 mm, which is acceptable for our application. This value is therefore selected, which ends the robot design with the proposed approach.
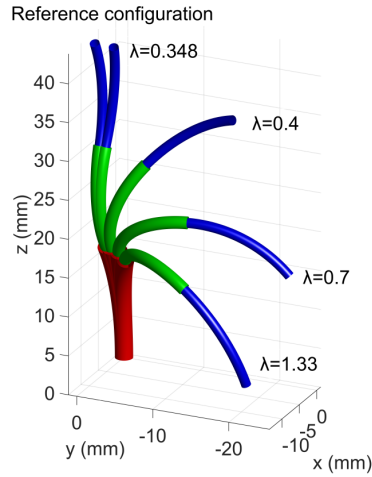
Reference configuration

Table 2: Tip position errors as a function of λ. $\lambda = 1.33$ corresponds to standard non-modified circular tubes.

λ	Tip position error (mm)
0.348	2.51
0.4	19.24
0.7	36.49
1.33	44.96

Fig. 3: Robot positions for different λ values.

Situation	A	B	C
Without error (mm)	0 (**0**)	0.79 (**0.27**)	2.51 (**0.95**)
With error (mm)	0 (**0**)	1.05 (**0.36**)	3.31 (**1.26**)

Table 3: Position errors during the follow-the-leader deployment. Maximum errors are in plain letters, RMS values are in bold.

4.3 Follow-the-leader behavior assessment

We now investigate precisely the follow-the-leader deployment errors by measuring tip position error and root mean square error along the robot's centerline for different deployment stages. The tubes are considered held at their insertion point. Measurements are reported in Table 3 with two indicators : the maximum error (Max), which is equal to the tip error, and the RMS value of deviation along the deployed robot. Three configurations during the deployment are considered : after deployment of the 3 tubes altogether (Point A, Fig. 1c), of tubes 1 and 2 altogether (Point B, Fig. 1c), and finally of tube 1 (Point C, Fig. 1c). At point A, errors are equal to zero. Further analysis shows that anisotropy leads to the existence of only one configuration, superimposed with the desired deployed geometry, a situation previously observed for two tubes in [10]. Results obtained are suitable for our application in terms of tip deviation.

In order to go further and explore the robustness of the follow-the-leader behavior, we introduce angular errors in the control of the tubes at their base. A value of 0.005 degree, achievable with standard encoders and transmissions, is chosen. Results in Table 3 indicate the maximum errors in presence of tube angular errors. Those results still remain acceptable for our application, which is encouraging and show the interest of the proposed robot design and deployment method.

5 Conclusion

In this paper, we have proposed a method for CTR design and deployment. It combines a simple kinematic approach and tube design to achieve approximate follow-the-leader deployment. We have shown that interesting accuracy can be obtained for a medical application. The effect of the actuation control errors on the robot deployment have also been studied, and we have demonstrated that such errors remain acceptable for our application. The interest of tube modification is outlined, with high sensitivity of the robot behavior to these modifications. Further work will now be focused on selecting the best tube patterning techniques to obtain anisotropic properties. Evaluation of sensitivity to design parameters and extension to other 3D deployment situations will also be considered.

Acknowledgment

References

1. Azimian, H., Francis, P., Looi, T., Drake, J.: Structurally-redesigned concentric-tube manipulators with improved stability. In: IEEE/RSJ International Conference on Intelligent Robots and Systems, pp. 2030–2035 (2014)
2. Bergeles, C., Gosline, A., Vasilyev, N., Codd, P., del Nido, P., Dupont, P.: Concentric tube robot design and optimization based on task and anatomical constraints. IEEE Transactions on Robotics **31**(1), 67–84 (2015)
3. Burgner-Kahrs, J., Rucker, D.C., Choset, H.: Continuum robots for medical applications: A survey. IEEE Transactions on Robotics **31**(6), 1261–1280 (2015)
4. Dupont, P., Lock, J., Butler, E.: Torsional kinematic model for concentric tube robots. In: IEEE International Conference on Robotics and Automation, pp. 3851–3858 (2009)
5. Dupont, P., Lock, J., Itkowitz, B., Butler, E.: Design and control of concentric-tube robots. IEEE Transactions on Robotics **26**(2), 209–225 (2010)
6. Gilbert, H., Neimat, J., Webster, R.: Concentric tube robots as steerable needles: Achieving follow-the-leader deployment. IEEE Transactions on Robotics **31**(2), 246–258 (2015)
7. Lee, D., Kim, J., Kim, J., Baek, C., Noh, G., Kim, D., Kim, K., Kang, S., Cho, K.: Anisotropic patterning to reduce instability of concentric-tube robots. IEEE Transactions on Robotics **31**(6), 1311–1323 (2015)
8. R. J. Webster, I., Romano, J.M., Cowan, N.J.: Mechanics of precurved-tube continuum robots. IEEE Transactions on Robotics **25**, 67–78 (2009)
9. Rucker, D.C.: The mechanics of continuum robots: Model–based sensing and control. Ph.D. thesis, Vanderbilt University (2011)
10. Rucker, D.C., R. J. Webster, I., Chirikjian, G.S., Cowan, N.J.: Equilibrium conformations of concentric-tube continuum robots. Int. J. of Robotics Research **29**, 1263–1280 (2010)